Research Article Vol. 9, No. 7 / 1 July 2019 / Optical Materials Express 3069
Optical Materials EXPRESS

Enhancing electrochemical properties of an ITO-coated lossy-mode resonance optical fiber sensor by electrodeposition of PEDOT:PSS

MICHAŁ SOBASZEK,[1] DARIUSZ BURNAT,[2] PETR SEZEMSKY,[3] VITEZSLAV STRANAK,[3] ROBERT BOGDANOWICZ,[1] MARCIN KOBA,[2,4] KATARZYNA SIUZDAK,[5] AND MATEUSZ ŚMIETANA[2,*]

[1]*Gdansk University of Technology, Faculty of Electronics, Telecommunications and Informatics, Department of Metrology and Optoelectronics, Narutowicza 11/12, 80-233 Gdansk, Poland*
[2]*Warsaw University of Technology, Faculty of Electronics and Information Technology, Institute of Microelectronics and Optoelectronics, Koszykowa 75, 00-662 Warszawa, Poland*
[3]*University of South Bohemia, Faculty of Science, Institute of Physics and Biophysics, Branisovska 1760, 370 05 Ceske Budejovice, Czech Republic*
[4]*National Institute of Telecommunications, Szachowa 1, 04-894 Warszawa, Poland*
[5]*Polish Academy of Sciences, The Szewalski Institute of Fluid-Flow Machinery, Fiszera 14, 80-231 Gdańsk, Poland*
[*]*M.Smietana@elka.pw.edu.pl*

Abstract: A sensor working in multiple domains may offer enhanced information about the properties of an investigated analyte, including those containing biological species. It has already been shown that a dual-domain sensing capability, i.e., in optical and electrochemical domains, can be offered by lossy-mode resonance (LMR) sensors based on indium-tin-oxide (ITO) thin film. The spectral response of the LMR sensors depends on the refractive index (RI) at the ITO surface. In this work, we discuss a capability for enhancing the electrochemical properties of these sensors by electrodeposition of poly(3,4-ethylenedioxythiophene)–poly(4-styrenesulfonate) (PEDOT:PSS) on the ITO surface. This conjugated polymer shows high electrical conductivity, high optical transmittance, as well as good chemical stability, and thus can be used as a transparent electrode. We have found that the PEDOT:PSS deposition improves the reversibility of the electrochemical reduction/oxidation reactions by 2.5 times with no negative impact on LMR-based measurements of the RI of the analyte.

1. Introduction

In recent years, increasing demand for novel diagnostic and analytical methods capable of investigating various biological targets at ultralow quantities has been observed [1]. When the label-free sensing concept is considered, where no fluorescent marker is applied and just binding phenomena between a biological receptor and a target at the sensor surface are monitored, the targets can be investigated in their natural state, and without a requirement for their additional modification or amplification. In the case of optical sensors, the label-free sensing concept relies on monitoring changes in the refractive index (RI) in the vicinity of the sensor surface [2]. An increase in RI corresponds to an increase in density, that is induced by biological binding events and can be monitored optically in real time [3].

Optical fiber sensors, due to their set of unique properties such as their small size, immunity to electromagnetic interference, and capability of multiparameter and remote sensing, have gathered significant attention of the scientific community. A number of optical fiber sensors capable of measurement of RI with high sensitivity have already been reported [4–6]. Due to their immunity to optical power fluctuations, sensors based on resonance effects such as surface plasmon resonance or lossy-mode resonance (LMR) [7–9] are desired. Among the advantages of

#364718 https://doi.org/10.1364/OME.9.003069
Journal © 2019 Received 19 Apr 2019; revised 29 May 2019; accepted 3 Jun 2019; published 20 Jun 2019

Optical Materials EXPRESS

LMR sensors is that many materials, which include metal and semiconductor oxides or nitrides, some carbon-based materials, as well as various polymers, can be used as thin films supporting the LMR effect [7,10,11]. An indium tin oxide (ITO) thin film deposited on fused silica glass may offer suitable properties for LMR observations. ITO is also well known for its low electrical resistivity, and due to its band-gap, it is often used as an electrochemical (EC) working electrode [12]. For this reason, ITO-based electrodes typically substitute those made of gold wherever optical absorption at the electrode surface needs to be monitored during the EC process [13]. In contrast to other transparent electrode materials, such as boron-doped diamond, thin ITO films can be deposited at a relatively low temperature on various substrates and shapes [14]. When ITO is used as an LMR-supporting thin film, a combined optical and EC analysis can be performed to deliver an enhanced set of data about the investigated analytes [3,15,16]. EC-enhanced optical measurements open up the possibility for detection of a variety of organic compounds and heavy metals, but also allow for sensor surface treatment in the EC domain, followed by optical detection. It is worth noting that tuning the properties of ITO to allow both high-quality LMR and EC response to be achieved is still challenging. The most recent reports of the EC response to the presence of a reduction/oxidation (redox) probe in a solution are unsatisfactory, i.e., weakly defined reduction (I_{red}) and oxidation (I_{ox}) current peaks were recorded using an ITO-LMR sensor [3,15,16]. Moreover, the difference in potentials corresponding to these peaks (ΔE) is significantly higher than observed for other commercially available electrodes, including those based on ITO. These parameters, namely I_{red}, I_{ox} and ΔE are crucial when label-free sensing applications in the EC domain are considered [17].

In this work, we propose electropolymerization of a conducting polymer on the ITO-coated optical fiber. The approach makes it possible to improve the EC properties of the device when the LMR effect has already been achieved. Poly(3,4-ethylenedioxythiophene)–poly(4-styrenesulfonate) (PEDOT:PSS) was chosen for electropolymerization by means of chronoamperometry (CA), and its further investigations were done with cyclic voltammetry (CV). PEDOT:PSS is a conjugated polymer showing high electrical conductivity (up to 550 S cm^{-1}) and good chemical stability in a doped state [18]. When polymerized as a thin film, PEDOT:PSS can be used as a transparent electrode with optical transmittance reaching up to 80% [19]. What is more, PEDOT:PSS is often used in various EC biosensors targeted towards e.g., pesticides [20], glucose [21], ascorbic acid [22] and dopamine [23]. In this work, we particularly focus on the influence of PEDOT:PSS electropolymerization on optical and EC properties of the ITO-LMR optical fiber sensor.

2. Experimental

2.1. ITO-LMR sensor fabrication and optical testing

The LMR structures were fabricated using approx. 15 cm-long 400/840 μm core/cladding diameter polymer-clad silica fiber samples, where 2.5 cm of polymer cladding was removed from the fiber central section [15]. Next, the electrically conductive and optically transparent ITO films were deposited by reactive magnetron sputtering of the ITO target (In_2O_3-SnO_2—90/10 wt % and a purity of 99.99%). The magnetron, whose axis was perpendicular to the substrate, was supplied by a Cito1310 (13.56 MHz, 300 W) RF source (Comet AG, Flamatt, Switzerland). The experiments were carried out at pressure $p = 0.1$ Pa in an argon atmosphere. The fibers were rotated in the chamber during the process to uniformly cover with ITO the exposed fiber core section.

To determine the RI sensitivity of the fabricated ITO-LMR devices, they were investigated in mixtures of water/glycerine with different proportions of these components resulting in n_D = 1.33–1.45 RIU. Before immersing the sensors in subsequent mixtures their RI was measured using an AR200 automatic digital refractometer (Reichert Inc., Buffalo, NY, USA). The RI sensing studies were conducted without any applied bias potential. The optical transmission of the ITO-LMR structure was interrogated in the range λ = 350–1050 nm using a HL-2000 white

Optical Materials EXPRESS

light source and a USB4000 spectrometer (Ocean Optics, USA). The optical transmission (T_i) in the specified spectral range was measured as counts in the specified integration time (up to 100 ms) and referred to the transmission of the fiber without the ITO coating (T_0). The results were normalized and presented as $T = T_i - T_0$. The temperature of the solutions was stabilized at 25 °C.

For the combined optical and EC analysis, the ITO-LMR sensor was installed in the measurement setup to record the T_i during each stage of the EC processing [15]. The T_i was monitored and the data were acquired approx. every 2 s. For comparison of the results, the following parameters were selected: (1) LMR wavelength (λ_R), and (2) T at the slope of the resonance at the arbitrary chosen λ=700 nm (T_{700}).

2.2. Electropolymerisation and EC setup

The CA processing and CV measurements were performed with a Palmsens Emstat 3+ potentiostat/galvanostat controlled by the PSTrace 5 software. We used the ITO-LMR sensor, a platinum wire, and Ag/AgCl/0.1 M KCl as the working (WE), counter (CE), and reference (REF) electrodes, respectively. The electropolymerization on ITO-LMR sensor was conducted by chronoamperometry by treated at constant potential 1.25 V vs. REF for 120 s in 0.1 M $NaSO_4$ containing 15 mM EDOT and 0.1 M PSS. The procedure allowed for electropolymerization of EDOT with a PSS counterion at the surface of the ITO-LMR sensor. The obtained at these conditions PEDOT:PSS film thickness may reach up to 800 nm [24,25]. The EC property, i.e., response to redox probes, before and after the electropolymerization was verified in 1 mM ferrocenedimethanol in 0.5 M Na_2SO_4 solution at a scan rate of 50 $mV \cdot s^{-1}$. The measurement cell used for the optical-EC investigation of the optical fiber sensor is shown schematically in Fig. 1.

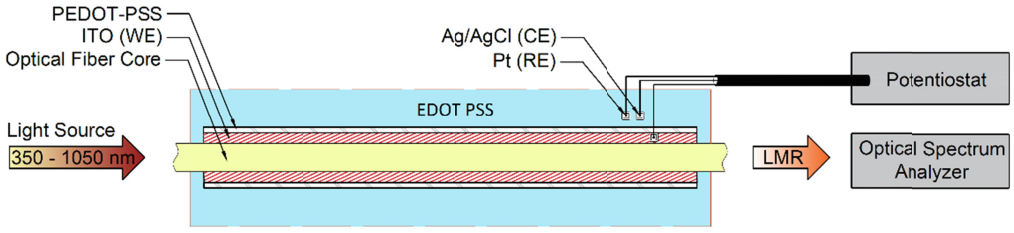

Fig. 1. Schematically shown experimental setup used for EDOT-PSS electropolymerization with optical monitoring of the ITO-LMR device.

The EC impedance spectroscopy (EIS) measurements were carried out to investigate process changes in space charge capacitance and resistance of charge transfer between the electrode and the electrolyte, whose detection is crucial. EIS is known for high precision and is frequently used to evaluate heterogeneous charge-transfer parameters and a double-layer structure [1]. During an EIS analysis, the impedance at a certain frequency (Z_i) is measured. When the WE is immersed in the electrolyte containing redox probe, it polarizes at the formal potential (E_f) of a particular redox reaction. The E_f, also known as the mid-peak potential, is defined as a half of the sum of the oxidation and reduction potential. For a reversible and diffusion-controlled redox reaction, at E_f the reduced and oxidized species diffuse at equal rates. Following that, EIS measurements were performed for ITO-coated and PEDOT:PSS-ITO-coated optical fiber structures at a determined E_f of ferrocenedimethanol redox reaction. The spectra were recorded in the frequency range 20 kHz – 0.1 Hz and with a 10 mV amplitude. The measured impedances were analyzed with an EIS Analyzer using an electric equivalent circuit (EEQC). The EEQC consists of different components, such as resistors, capacitors, a coil or Warburg elements of features, that correspond to the real processes occurring at the electrode/electrolyte interface. In other words, the EEQC

Optical Materials EXPRESS

shows the same electrical response as the WE. A modified Powell algorithm [26] was used with an amplitude weighting r_a as in Eq. 1, where N is the number of points, M is the number of parameters, ω is the angular frequency, and $P_1 \ldots P_M$ are model parameters. The r_c is defined as in Eq. 2, where i corresponds to the measured values of impedance, and i_{calc} is attributed to the calculated values.

$$r_a = (\omega, P_1 \ldots P_M) = r_c^2/(N - M) \tag{1}$$

$$r_c^2 = \sum_{i=1}^{N} \frac{(Z'_i - Z'_{i_{calc}})^2 + (Z''_i - Z''_{i_{calc}})^2}{Z'^2_i + Z'^{\,2}_{i_{calc}}} \tag{2}$$

3. Result and discussion

Before the EDOT-PSS electropolymerization, the response of the ITO-LMR sensor to the applied potential was verified. The attenuation band in the monitored spectrum is originated by a resonance effect. The LMR is dependent on the thin film thickness since the thickness determines propagation conditions for the lossy modes [27]. In can be seen in Fig. 2 that during CV measurements, the optical spectrum did not experience any significant alterations. The corresponding CV curve is shown in Fig. 4A. For a better insight, in Fig. 2C both the λ_R and T_{700} were plotted vs. the measurement number that corresponds to the applied potential. During the measurements, λ_R stayed almost constant, which means that there was no influence of the potential on the LMR. For the previously investigated ITO-LMR sensors [12–14], where ITO was deposited at a higher pressure, it was shown that the changes in applied potential had a significant impact on the LMR. The negligible influence observed here corresponds to the properties of the ITO coating deposited at a lower pressure, i.e., the ITO layer contains more crystalline forms, so its bandgap is different than for ITO deposited at a higher pressure [28]. Moreover, the lack of potential influence can be explained by a mismatch between energy levels for ITO and the ferrocenedimethanol redox probe [16]. The simultaneously recorded EC response for one of the cycles is shown in Fig. 4, and it will be discussed later together with the results obtained after the electropolymerization.

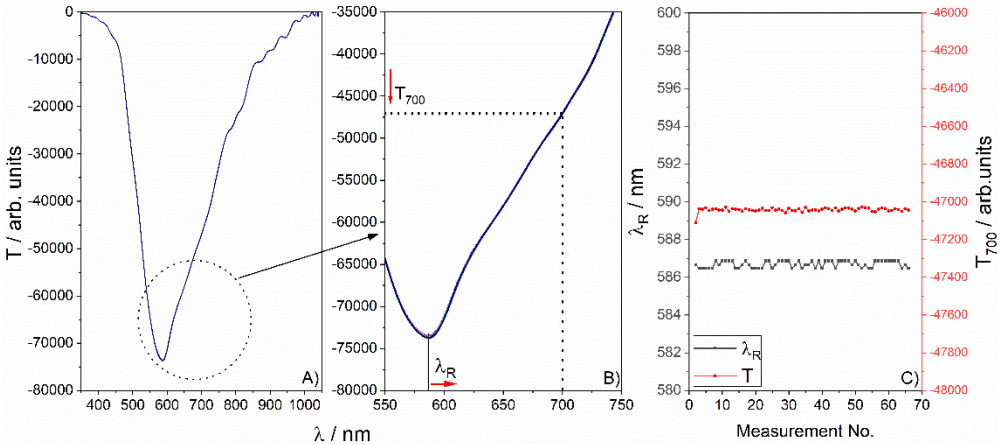

Fig. 2. Optical response of the ITO-LMR sensor to potential scanning (4 scans) with scan rate 50 mV/s in 1 mM ferrocenedimethanol in 0.1M KCl, where (A) shows spectrum presented as $T = T_i - T_0$, where T_i and T_0 are the optical transmissions of the ITO coated and uncoated fiber respectively, (B) magnification of selected part of the spectrum with shown evolution of T_{700} and λ_R, and (C) resonance wavelength and T at λ=700 nm for all the measurements.

Optical Materials EXPRESS

Table 1. Oxidation and reduction potentials and currents obtained for CV recorded in 1 mM ferrocenedimethanol in 0.1M KCl with the ITO-LMR sensor before and after PEDOT:PSS deposition.

Sample	E_{ox} [V]	E_{red} [V]	$\Delta E = E_{ox} - E_{red}$ [V]	I_{ox} [μA]	I_{red} [μA]
ITO-LMR	0.485	−0.025	0.51	20	16
PEDOT:PSS/ITO-LMR	0.311	0.101	0.21	73	71

Next, electropolymerization of EDOT was performed on the ITO-LMR sensor. Its optical response during the process is shown in Fig. 3. Significant alteration of the spectrum can be observed. The λ_R, initially at 578.56 nm, gradually shifts within 60 s (approx. 30 initial measurements) towards longer wavelengths reaching 594.73 nm ($\Delta\lambda_R = 16.17$ nm). The T_{700} follows the trend for λ_R. After the initial 60 s, a significantly lower influence of the process on the T_{700} was observed too (Fig. 3(C)). The results confirm the PEDOT:PSS film deposition on the ITO-LMR sensors, i.e., a direction of the shift corresponds to an increase in RI at the ITO surface, which is followed by deposition of the film [3]. It must be noted that mainly the right slope of the resonance is influenced by the deposition. The effect may be caused by non-uniform polymer deposition around the fiber, possibly induced by some distribution in the ITO resistivity. Non-uniform coating distribution around the fiber may induce asymmetrical mode coupling and thus less pronounced resonances are observed in the transmission spectrum [29].

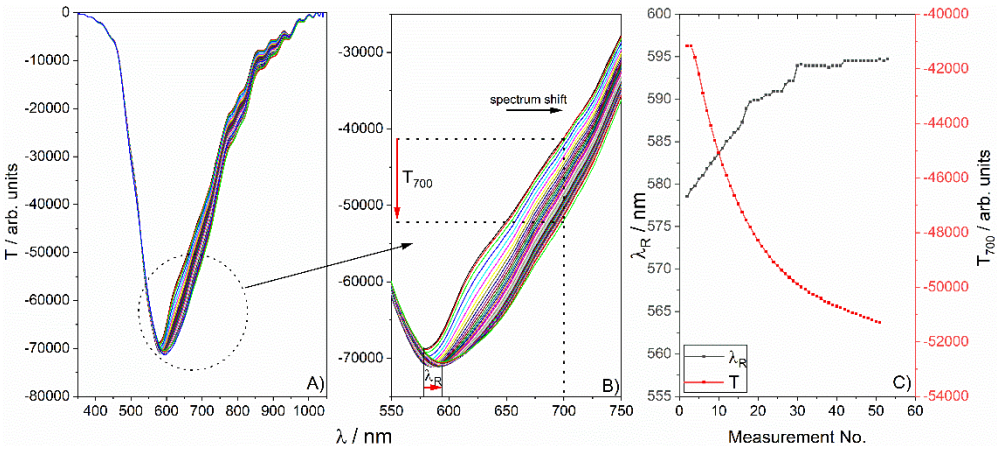

Fig. 3. Optical response of the ITO-LMR sensor to EDOT electropolymerization in 0.5 Na_2SO_4 at 1.25 V during a 120 s long process, where (A) shows the evolution of the spectrum, (B) magnification of selected part of the spectrum with shown evolution of T_{700} and λ_R, and (C) the shift of the resonance wavelength and T at $\lambda = 700$ nm.

CV is an EC technique often used for verification of changes at an electrode surface. PEDOT:PSS electrode typically exhibits wide potential range of c.a. 1-1.5 V, but it concerns the full range when this electrode works in a buffer solution. In the case of the electrode immersed in an electrolyte containing ferrocyanide redox probe, the difference between oxidation and reduction peaks reaches 450 mV or even 200 mV [30]. Low ΔE is attributed to improved conductivity and mass transfer between redox species and surface of the polymer electrode [31,32]. Hence, the EC properties of the ITO-LMR sensor before and after electropolymerization were compared (Fig. 4(A)). For the sensor, prior to the electropolymerization, reversible reduction and oxidation peaks corresponding to one electron process are not well-defined, and $\Delta E = 510$ mV. As a result of the electropolymerization process, ΔE has been reduced by factor of 2.4, reaching $\Delta E = 210$ mV. A similar ΔE value is often achieved for glassy carbon, boron-doped diamond or gold electrodes

Optical Materials EXPRESS

[12,33]. For commercially available ITO films deposited on glass slides, ΔE is close to 100 mV. It must also be emphasized that the polymer deposition resulted in better definition of both I_{ox} and I_{red}, which are higher for the sensor coated with PEDOT:PSS. The absolute values of the currents are nearly equal, which indicates a high reversibility of the redox reaction. The key EC parameters received from the CV curves are summarized in Table 1.

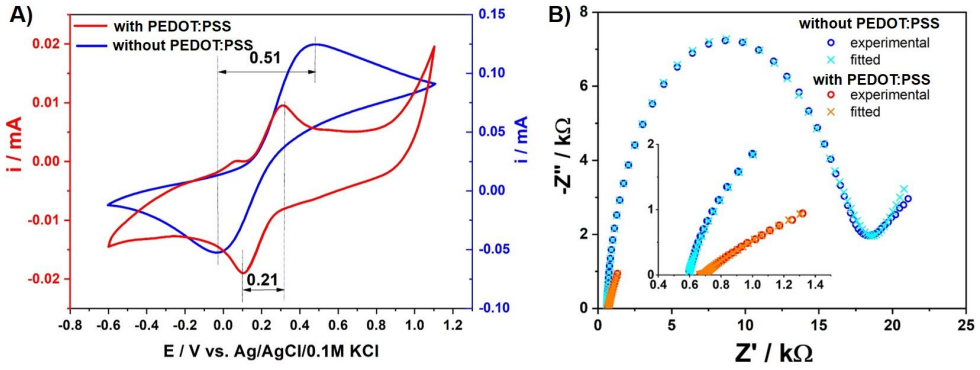

Fig. 4. (A) CV recorded in 1 mM ferrocenedimethanol in 0.1 M KCl with the ITO-LMR sensor before and after PEDOT:PSS deposition. The potential and currents corresponding to redox peaks are indicated in Table 1. (B) EIS response recorded at the redox formal potential for ITO-LMR sensor with and without PEDOT:PSS coating. The inset in (B) is a close-up of the initial part of the figure.

Additionally, at the E_f of the redox reaction, EIS was also recorded and presented in Fig. 4(B). When bare ITO was interfacing the electrolyte containing the redox probe, a semicircle initially with a 45° slope was observed. After deposition of the PEDOT:PSS, the response changed significantly and the overall impedance decreased. As already mentioned in the experimental section, to better understand the impedance data, EIS modelling was performed. The EEQC proposed for both cases is presented in Fig. 5. According to the applied EEQC including both of the electrode materials, goodness was at the level of 10^{-5}, whereas the error at each element value did not exceed several %, which is proof of the correctness of the designed circuit.

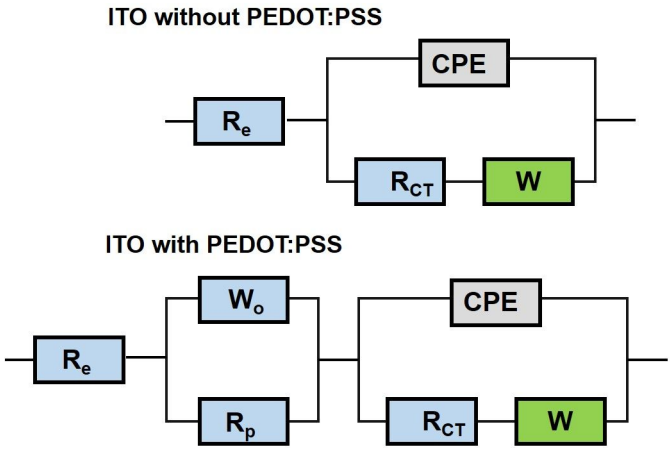

Fig. 5. The EEQC used for fitting of the EIS data received with and without PEDOT:PSS film.

Optical Materials EXPRESS

The designed EEQC consists of the following components: i) resistances: R_e - attributed to the electrolyte resistance, R_p – the polymer resistance itself, R_{CT} - charge transfer resistance, ii) constant phase element (CPE) that models the behavior of a double layer, and iii) two Warburg-like components, which will be discussed later. Independently on the investigated working electrode, the electrolyte resistance is at the same level, and equals to 590 Ω and 667 Ω for ITO and ITO/PEDOT:PSS, respectively. The difference may result from some slight changes in the geometric arrangement of electrodes for both the cases, but it does not impact on the overall impedance value.

The CPE is attributed to the space charge capacitance, and its impedance is described by $Z = Q^{-1}(i\omega)^{-m}$, where Q is a CPE parameter, m is exponential and in both cases reaches c.a. 0.9. According to Bard *et al.* [34], for $m = 1$, it stands for an ideal capacitance, while for $m = 0.5$ indicates highly dispersed capacitance, that is typical for porous electrodes. The Warburg component labelled as W represents the impedance of semi-infinite diffusion to/from a flat electrode. This component contributes equally to the real (ReZ) and imaginary (ImZ) parts of the impedance: $ReZ(\omega) = A_W/\omega^{0.5}$ and $ImZ(\omega) = -A_W/\omega^{0.5}$, where A_W is the Warburg coefficient.

In comparison to the bare ITO, for a PEDOT:PSS-coated substrate, the EEQC includes an additional section consisting of W_o and R_p, where they represent finite length diffusion at a reflective boundary and ω_{or} stands for the Warburg coefficient, whereas $W_{OC} = d/D^{0.5}$. The impedance of the W_o component is given by Eq. 3. W_o is typically applied for modelling of diffusion processes occurring in a polymer matrix and sometimes is termed subdiffusion impedance [35].

$$Z_{W_0}(\omega) = \frac{\omega_{or}}{\sqrt{\omega}}(1 - j)\coth[W_{OC}\sqrt{j\omega}] \tag{3}$$

The difference between both of the electrode materials can be seen when the EEQC segment attributed to the charge transfer is considered. The values for those elements are listed in Table 2. The ITO/PEDOT:PSS electrode exhibits much higher capacitance and lower charge transfer resistance, while the Warburg diffusion is 2.6 times lower for the electrode coated with ITO only. The PEDOT:PSS film enhances the transfer of electric charges between the electrolyte and ITO. Therefore, the presence of PEDOT:PSS significantly enhances the EC response.

Table 2. The values of EEQC parameters responsible for charge transfer and diffusion.

Element / Unit	ITO	ITO/PEDOT:PSS
CPE / $\Omega^{-1}s^n$	1.76×10^{-5} ($m = 0.86$)	5×10^{-4} ($m = 0.91$)
R_1 / Ω	2608.2	1.5
W / Ω $s^{-0.5}$	2399.8	912.7

The PEDOT:PSS/ITO-LMR sensor, simultaneously to EC interrogation, was again tested optically (Fig. 6). Afterwards, the film deposition alterations in the spectrum are more intense when compared to those before the deposition. Both the λ_R and T_{700} respond to the applied potential. The λ_R reaches its maximum and minimum for 0.1 V and 0.3 V applied potential, respectively, while the relation for T_{700} is inverted due to its location on the right slope of the resonance. This phenomenon can be explained by modulation of the RI of the ITO, which is an n-type semiconductor when charges are delivered, and changes in RI of the solution at the sensor surface when ions from the electrolyte are attracted or pushed away from the sensor surface [16]. After the PEDOT:PSS deposition, the charge transfer because of substantial resistances R and W decrease, as indicated in Table 2.

Finally, the optical response to RI changes at the PEDOT:PSS/ITO-LMR sensor has been verified. For any label-free sensing applications, the sensor must be sensitive to RI changes at its surface. As shown in [15–16], ITO–LMR optical fiber sensors without additional coatings are suitable for this application. To preserve the possibility of multiple domain detection the

Optical Materials EXPRESS

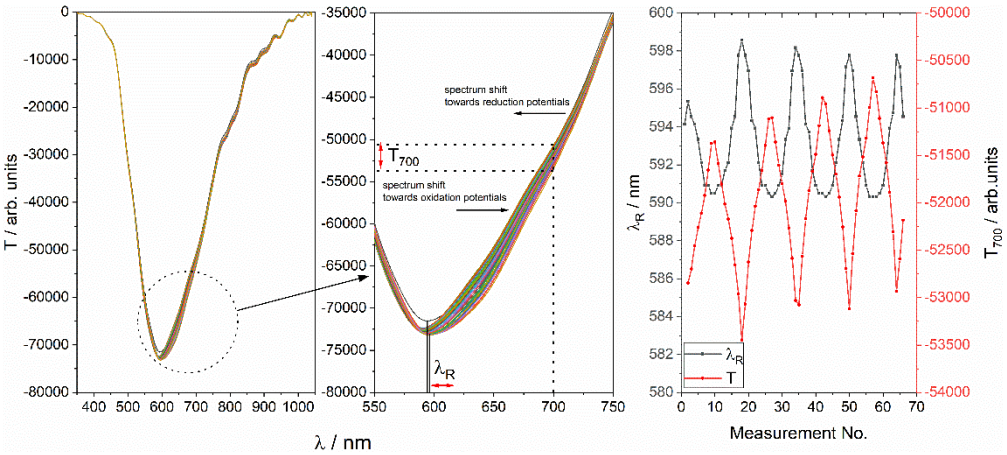

Fig. 6. Optical response of the PEDOT:PSS/ITO-LMR sensor to potential scanning (4 scans) at a rate of 50 mV/s in 1 mM ferrocenedimethanol in 0.1M KCl, where (A) shows the evolution of the spectrum, (B) magnification of selected part of the spectrum with shown evolution of T_{700} and λ_R, and (C) the shift of resonance wavelength and T at λ=700 nm.

optical response of the PEDOT:PSS/ITO-LMR sensor must not be disturbed. In Fig. 7(A), a well-defined LMR can be seen. It experiences a shift towards higher wavelengths when the RI increases. Referring to spectra presented above, measured in the electrolytes with redox probes or EDOT and PSS, the resonance is initially shifted towards shorter wavelengths due to the lower RI of the external medium. The significant response to RI after the electropolymerization proves that the PEDOT:PSS does not disturb the optical sensing effect, i.e., the surface is not blocked by the polymer films and does not prevent interactions with an external medium.

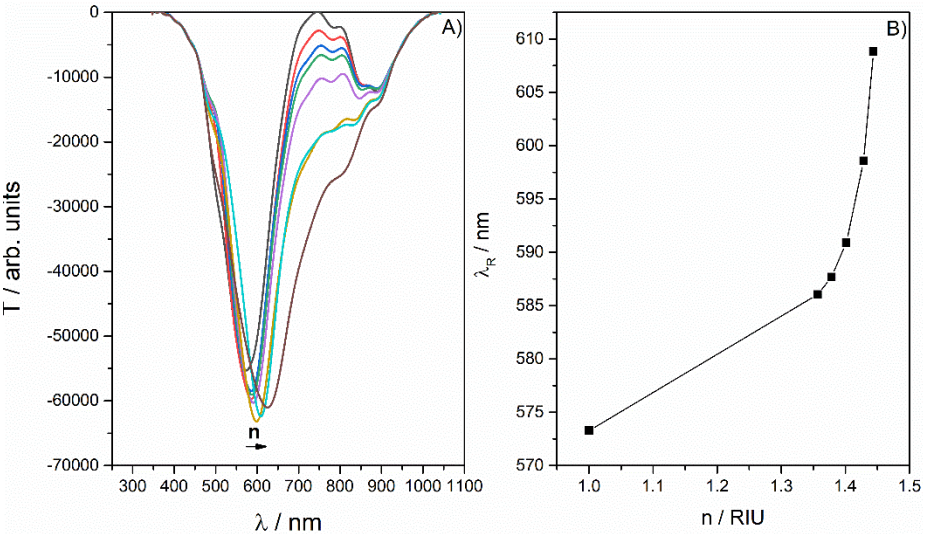

Fig. 7. Optical response of the PEDOT:PSS/ITO-LMR sensor to external RI (n), where (A) shows evolution of the spectrum, and (B) shift in the resonance wavelength.

Optical Materials EXPRESS

4. Conclusion

We investigated the possibility to enhance the sensing properties of an ITO-LMR sensor by electropolymerization of PEDOT:PSS on ITO surface. As a result of the process the reduction-oxidation peak-to-peak separation was significantly reduced, and the current peaks became more pronounced. Most importantly, after the PEDOT:PSS deposition, the sensor still stayed sensitive to external refractive index. This fact allows such an approach to be considered as suitable for improving the properties of opto-electrochemical label-free sensors. The deposition of a conducting polymer like PEDOT:PSS is a low-cost solution to enhance the electrochemical properties of the ITO-LMR devices.

Funding

Narodowe Centrum Nauki (NCN) (2014/14/E/ST7/00104, 2016/21/B/ST7/01430); Narodowe Centrum Badań i Rozwoju (NCBR) (347324/12/NCBR/2017); North Atlantic Treaty Organization (NATO) (SPS G5147).

Disclosures

The authors declare that there are no conflicts of interest related to this article.

References

1. D. Nidzworski, K. Siuzdak, P. Niedziałkowski, R. Bogdanowicz, M. Sobaszek, J. Ryl, P. Weiher, M. Sawczak, E. Wnuk, W. A. Goddard, A. Jaramillo-Botero, and T. Ossowski, "A rapid-response ultrasensitive biosensor for influenza virus detection using antibody modified boron-doped diamond," Sci. Rep. **7**(1), 15707 (2017).
2. J. E. Antonio-Lopez, J. J. Sanchez-Mondragon, P. LiKamWa, and D. A. May-Arrioja, "Fiber-optic sensor for liquid level measurement," Opt. Lett. **36**(17), 3425–3427 (2011).
3. R. Bogdanowicz, P. Niedziałkowski, M. Sobaszek, D. Burnat, W. Białobrzeska, Z. Cebula, P. Sezemsky, M. Koba, V. Stranak, T. Ossowski, and M. Śmietana, "Optical Detection of Ketoprofen by Its Electropolymerization on an Indium Tin Oxide-Coated Optical Fiber Probe," Sensors **18**(5), 1361 (2018).
4. D. K. C. Wu, B. T. Kuhlmey, and B. J. Eggleton, "Ultrasensitive photonic crystal fiber refractive index sensor," Opt. Lett. **34**(3), 322–324 (2009).
5. M. Janik, A. K. Myśliwiec, M. Koba, A. Celebańska, W. J. Bock, and M. Śmietana, "Sensitivity Pattern of Femtosecond Laser Micromachined and Plasma-Processed In-Fiber Mach-Zehnder Interferometers, as Applied to Small-Scale Refractive Index Sensing," IEEE Sens. J. **17**(11), 3316–3322 (2017).
6. M. Śmietana, M. Koba, P. Mikulic, and W. J. Bock, "Towards refractive index sensitivity of long-period gratings at level of tens of μm per refractive index unit: fiber cladding etching and nano-coating deposition," Opt. Express **24**(11), 11897–11904 (2016).
7. I. D. Villar, C. R. Zamarreño, M. Hernaez, F. J. Arregui, and I. R. Matias, "Lossy Mode Resonance Generation With Indium-Tin-Oxide-Coated Optical Fibers for Sensing Applications," J. Lightwave Technol. **28**(1), 111–117 (2010).
8. N. Paliwal and J. John, "Lossy Mode Resonance (LMR) Based Fiber Optic Sensors: A Review," IEEE Sens. J. **15**(10), 5361–5371 (2015).
9. Q. Wang and W.-M. Zhao, "A comprehensive review of lossy mode resonance-based fiber optic sensors," Opt. Lasers Eng. **100**, 47–60 (2018).
10. M. Śmietana, M. Dudek, M. Koba, and B. Michalak, "Influence of diamond-like carbon overlay properties on refractive index sensitivity of nano-coated optical fibres," Phys. Status Solidi A **210**(10), 2100–2105 (2013).
11. K. Kosiel, M. Koba, M. Masiewicz, and M. Śmietana, "Tailoring properties of lossy-mode resonance optical fiber sensors with atomic layer deposition technique," Opt. Laser Technol. **102**, 213–221 (2018).
12. J. Stotter, Y. Show, S. Wang, and G. Swain, "Comparison of the Electrical, Optical, and Electrochemical Properties of Diamond and Indium Tin Oxide Thin-Film Electrodes," Chem. Mater. **17**(19), 4880–4888 (2005).
13. J. Agrisuelas, D. Giménez-Romero, J. J. García-Jareño, and F. Vicente, "Vis/NIR spectroelectrochemical analysis of poly-(Azure A) on ITO electrode," Electrochem. Commun. **8**(4), 549–553 (2006).
14. D. C. Paine, T. Whitson, D. Janiac, R. Beresford, C. O. Yang, and B. Lewis, "A study of low temperature crystallization of amorphous thin film indium–tin–oxide," J. Appl. Phys. **85**(12), 8445–8450 (1999).
15. M. Śmietana, M. Sobaszek, B. Michalak, P. Niedziałkowski, W. Białobrzeska, M. Koba, P. Sezemsky, V. Stranak, J. Karczewski, T. Ossowski, and R. Bogdanowicz, "Optical Monitoring of Electrochemical Processes With ITO-Based Lossy-Mode Resonance Optical Fiber Sensor Applied as an Electrode," J. Lightwave Technol. **36**(4), 954–960 (2018).
16. M. Śmietana, P. Niedziałkowski, W. Białobrzeska, D. Burnat, P. Sezemsky, M. Koba, V. Stranak, K. Siuzdak, T. Ossowski, and R. Bogdanowicz, "Study on Combined Optical and Electrochemical Analysis Using Indium-tin-oxide-coated Optical Fiber Sensor," Electroanalysis **31**(2), 398–404 (2019).

Optical Materials EXPRESS

17. G. Li, Z. Li, X. You, J. Chen, and S. Tang, "A novel label-free and sensitive electrochemical biosensor for Hg2+ based on ligase-mediated formation of DNAzyme," Talanta **161**, 138–142 (2016).
18. L. A. A. Pettersson, F. Carlsson, O. Inganäs, and H. Arwin, "Spectroscopic ellipsometry studies of the optical properties of doped poly(3,4-ethylenedioxythiophene): an anisotropic metal," Thin Solid Films **313-314**, 356–361 (1998).
19. Y. Chen, K. S. Kang, K. J. Han, K. H. Yoo, and J. Kim, "Enhanced optical and electrical properties of PEDOT: PSS films by the addition of MWCNT-sorbitol," Synth. Met. **159**(17-18), 1701–1704 (2009).
20. G. Istamboulie, T. Sikora, E. Jubete, E. Ochoteco, J.-L. Marty, and T. Noguer, "Screen-printed poly(3,4-ethylenedioxythiophene) (PEDOT): A new electrochemical mediator for acetylcholinesterase-based biosensors," Talanta **82**(3), 957–961 (2010).
21. J. Park, H. K. Kim, and Y. Son, "Glucose biosensor constructed from capped conducting microtubules of PEDOT," Sens. Actuators, B **133**(1), 244–250 (2008).
22. A. Bello, M. Giannetto, G. Mori, R. Seeber, F. Terzi, and C. Zanardi, "Optimization of the DPV potential waveform for determination of ascorbic acid on PEDOT-modified electrodes," Sens. Actuators, B **121**(2), 430–435 (2007).
23. K.-C. Lin, T.-H. Tsai, and S.-M. Chen, "Performing enzyme-free H2O2 biosensor and simultaneous determination for AA, DA, and UA by MWCNT–PEDOT film," Biosens. Bioelectron. **26**(2), 608–614 (2010).
24. B. Friedel, P. E. Keivanidis, T. J. K. Brenner, A. Abrusci, C. R. McNeill, R. H. Friend, and N. C. Greenham, "Effects of Layer Thickness and Annealing of PEDOT:PSS Layers in Organic Photodetectors," Macromolecules **42**(17), 6741–6747 (2009).
25. A. U. Palma-Cando, B. A. Frontana-Uribe, J. L. Maldonado, and M. R. Hernández, "Control of Thickness of PEDOT Electrodeposits on Glass/ITO Electrodes from Organic Solutions and its Use as Anode in Organic Solar Cells," Procedia Chem. **12**, 92–99 (2014).
26. L. Lu, B. H. Brown, D. C. Barber, and A. D. Leathard, "A fast parametric modelling algorithm with the Powell method," Physiol. Meas. **16**(3A), A39–A47 (1995).
27. I. Del Villar, M. Hernaez, C. R. Zamarreño, P. Sánchez, C. Fernández-Valdivielso, F. J. Arregui, and I. R. Matias, "Design rules for lossy mode resonance based sensors," Appl. Opt. **51**(19), 4298–4307 (2012).
28. L. Meng and M. P. dos Santos, "Properties of indium tin oxide (ITO) films prepared by r.f. reactive magnetron sputtering at different pressures," Thin Solid Films **303**(1-2), 151–155 (1997).
29. P. Zubiate, C. R. Zamarreño, I. D. Villar, I. R. Matias, and F. J. Arregui, "Experimental Study and Sensing Applications of Polarization-Dependent Lossy Mode Resonances Generated by D-Shape Coated Optical Fibers," J. Lightwave Technol. **33**(12), 2412–2418 (2015).
30. F. Abd-Wahab, A. Guthoos, H. Farhana, W. Salim, and W. W. Amani, "Solid-State rGO-PEDOT:PSS Transducing Material for Cost-Effective Enzymatic Sensing," Biosensors **9**(1), 36 (2019).
31. Y. Hui, C. Bian, J. Wang, J. Tong, and S. Xia, "Comparison of Two Types of Overoxidized PEDOT Films and Their Application in Sensor Fabrication," Sensors **17**(3), 628 (2017).
32. A. Benoudjit, M. M. Bader, and W. W. A. W. Salim, "Study of electropolymerized PEDOT:PSS transducers for application as electrochemical sensors in aqueous media," Sensing and Bio-sensing Research **17**, 18–24 (2018).
33. G. M. Swain and R. Ramesham, "The electrochemical activity of boron-doped polycrystalline diamond thin film electrodes," Anal. Chem. **65**(4), 345–351 (1993).
34. A. J. Bard and L. R. Faulkner, *Electrochemical Methods: Fundamentals and Applications*, 2nd edition (Wiley, 2000).
35. E. Hernández-Balaguera, H. Vara, and J. L. Polo, "An electrochemical impedance study of anomalous diffusion in PEDOT-coated carbon microfiber electrodes for neural applications," J. Electroanal. Chem. **775**, 251–257 (2016).